Mesoscale liquid model of chromatin recapitulates large-scale organization of eukaryotic cell nuclei.

Rabia L Laghmach[1], Michele Di Pierro[2], and Davit A Potoyan[1,3]✉

[1]Department of Chemistry, Iowa State University Ames IA
[2]Center for Theoretical Biological Physics, Rice University Houston TX
[3]Department of Biochemistry and Molecular Biology, Iowa State University Ames IA

Abstract

The nuclear envelope segregates the genome of eukaryota from the cytoplasm. Within nucleus chromatin is further compartmentalized into architectures that change throughout lifetime of the cell. Epigenetic patterns along the chromatin polymer strongly correlate with chromatin compartmentalization and, accordingly, also change during cell life cycle and at differentiation. Recently, it has been suggested that sub-nuclear chromatin compartmentalization might result from a process of liquid-liquid phase separation orchestrated by the epigenetic marking and operated by proteins that bind to chromatin. Here, we translate these observations into a diffuse interface model of chromatin, which we named Mesoscale Liquid mOdel of Nucleus (MELON). Using this streamlined continuum model of the genome, we study the large-scale rearrangements of chromatin that happen at different stages of the growth and senescence of the cell, and during nuclear inversion events. Particularly, we investigate the role of droplet diffusion, fluctuations, and heterochromatin-lamina interactions during nuclear remodeling. Our results indicate that the physical process of liquid-liquid phase separation, together with surface effects is sufficient to recapitulate much of the large-scale morphology and dynamics of chromatin along the life cycle of cells.

Chromatin| Eukaryotic Nucleus | Meso-scale modeling | phase separation |
Correspondence: ***potoyan@iastate.edu***

Introduction

Functional compartmentalization is a ubiquitous hallmark of life; by segregating bio-molecules and their interactions cells achieve specialization and improved efficiency of many of their functions (1, 2). In eukaryotic cells, the genetic material is separated from the cytoplasm by the nuclear membrane within the few cubic micrometers of nuclear space. Within the nuclear boundary, we find further compartmentalization which, however, exists in the absence of membranes (3). The structural organization of chromosomes changes with the cell type and phase of life, chromosomal loci have been observed to move across genomic compartments during cell differentiation. As a consequence, chromatin compartmentalization is believed to play a role in gene regulation and in the definition of cellular phenotypes (4, 5).

The first evidence of chromatin sub-nuclear organization in interphase was the discovery of the nucleolus in the early nineteenth century, followed by the discovery of regions in the nucleus with distinct optical properties, which were named heterochromatin and euchromatin (6). Heterochromatin appears dense and slow diffusing, containing regions of chromosomes corresponding to mostly silenced genes. Euchromatin, on the other hand, appear less dense and more mobile, composed of mostly active genes (7, 8). The latest electron microscopy tomography experiments have confirmed the DNA density variations between heterochromatic and euchromatic regions without, however, finding any structural difference between the two types of chromatin (9).

Clear evidence of hierarchical compartmentalization in chromatin at multiple scales have emerged through studies employing DNA-DNA proximity ligation assays. First, two genomic compartments were observed (3), named A and B which were then refined through higher resolution experiments to reveal the existence of even smaller subcompartments (5). The A and B compartments appear to be enriched in epigenetic markings correlating with transcriptional activation and silencing respectively. Several studies have suggested that chromatin compartmentalization might results from a process of liquid-liquid phase separation orchestrated by the epigenetic marking and operated by proteins that bind along the DNA polymer (10–15).

Chromatin compartmentalization is also consistent with recent experiments that have revealed the remarkable ability of intrinsically disordered proteins to phase separate and form liquid-like protein-rich droplets (16–19). Akin to oil droplets in a well shaken bottle of vinaigrette the protein rich droplets can appear and disappear according to external triggers, can divide and undergo fusion forming larger droplets (20–22). Most importantly, in the latest series of experiments, members of the family of HP1 proteins (Heterochromatin protein 1) known for regulation of heterochromatin content in the nucleus have been shown to undergo liquid-liquid phase separation both *in vivo* and *in vitro* under variety of conditions (23, 24). Consequently, protein-induced phase separation of chromosomal domains might constitute a direct physical mechanism for regulating genetic processes in space and time in the nucleus (16, 25).

The global architecture of chromosomes appears indeed to be determined by the interplay between chromatin phase separation and motor activity (10–12, 26, 27). Besides chromatin compartmentalization, the other prominent feature of genome three-dimensional architecture, the topologically associated domains (TADs), also appear to arise through either or both the processes of phase separation and DNA extrusion (28). Theoretical models based on polymer dynamics have been successfully used to connect one-dimesional epigenetic information to the three-dimensional architecture of the genome. Indeed, it is possible to predict the structural ensembles of human chromosomes with high accuracy based exclusively on information extracted from chromatin immuno-precipitation sequencing (ChIP-seq) (11). The same theoretical framework, composed exclusively of polymer connectivity, motor activity and micro-phase separation was shown to successfully explains a wide range of experimental observations about the dynamics of chromosomal loci (12). The sub-diffusive behavior of chromatin together with the heterogeneity of the individual diffusing trajectories (29), the viscoelasticity of the nuclear environment (30) , and the coherent motion of DNA observed by correlation spectroscopy (31) were all naturally predicted through theoretical and computational modelling.

Here we set out to investigate the specific contribution of liquid-liquid phase separation to genome architecture and separate its effects from those of polymer connectivity and motor activity. To gain insights into the roles of phase separation and surface effects in chromatin compartmentalization, we introduce the MEsoscale Liquid mOdel of Nucleus (MELON), a physical model of nuclear organization which is rooted in the theory of complex fluids. We use diffuse interface finite element simulations to model the evolution of nuclear chromatin compartments under various developmental processes including growth and inversion/senescence. Our approach draws inspiration and integrates elements of several mesoscopic cellular models such as the two-fluid hydrodynamic model of chromatin (32), the multi-cellular growth model (33, 34), the polymer models with epigenetic coloring already mentioned and active cellular mechanics (35–37). We apply MELON framework for modeling liquid-liquid phase separation driven reorganization of chromatin compartments in *Drosophila melanogaster* nucleus under wide variety of conditions including both equilibrium and non-equilibrium nuclear remodeling. The generic nature of the MELON model and the minimal assumptions that we have built into it, however, allow us to draw conclusion on the physical nature of chromatin reorganization which should be generally applicable for wide variety of eukaryotic nuclei beyond the specific case of *Drosophila*.

The meso-scale liquid model of the nucleus (MELON)

In this section, we present the basic physics and motivating biology behind the MEsoscale Liquid mOdel of Nucleus (MELON). More details about the mathematical formulation and computational implementation of MELON can be found in the Supporting Information. The MELON is set up to model the micron scale liquid dynamics and epigenetically orchestrated liquid-liquid phase separation of chromatin compartments in the nucleus. To this end, we construct the global free energy functional based on essential physical features: phase separation, surface tension, volume constraints and specific interaction of chromatin types. The nuclear chromatin morphology is defined through fluctuating order parameters which resolve (i) Nuclear membrane $\phi_0(r,t)$ (ii) Global $i = 1,...,N$ chromosome territories $\phi_i(r,t)$ and (iii) Epigenetic states of chromatin $\psi(r,t)$ which smoothly varies from 0 to 1 corresponding to A and B chromatin types respectively (Fig 1).

The time evolution of all the order parameters is governed by a global free energy functional. The specific forms of the free energy functional terms are motivated either by basic experimental facts about the chromosomal organization (existence of territories and types) or polymeric physics of chromosomes (excluded volume, de-mixing of types). The mesoscale resolution of chromatin naturally addresses the questions of epigenetically driven liquid-liquid phase separation, surface effects of chromatin compartment formation as well as diffusion and fluctuations of chromocenters and liquid chromatin droplets within the nucleus.

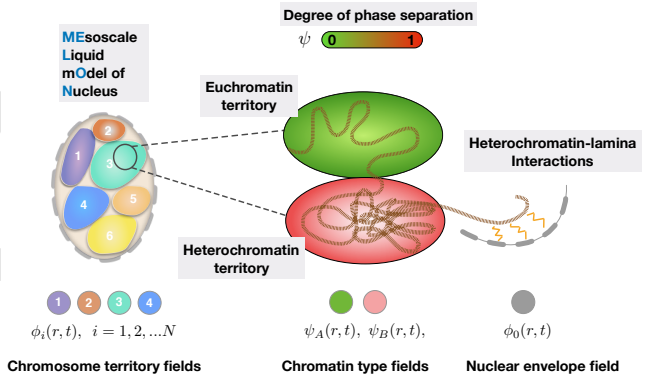

Fig. 1. Illustration of the MELON framework. Nucleus is resolved by several marginally overlapping liquid-like chromosomal territories each of which is described by an individual field variable. Within each chromosomal territory, we introduce an additional variable describing (possible) chromatin phase separation into A/B types that form hetero or eu-chromatin droplets. A separate field variable is introduced for describing the elastic membrane and its relaxation dynamics during the events of nuclear growth or inversion.

After all the relevant interactions are accounted, the steady-state nuclear morphology is generated by a stochastic search for the global minimum of the free energy functional in the space of phase-field variables $\boldsymbol{\varphi} = \{\varphi_0, \{\phi_i\}_{i=1,...,N}, \psi\}$:

$$F[\boldsymbol{\varphi}] = F_B[\boldsymbol{\varphi}] + F_R[\boldsymbol{\varphi}] + F_G[\boldsymbol{\varphi}] + F_I[\varphi_0, \psi] \qquad \textbf{(1)}$$

The base free energy term F_B accounts for surface energy contribution of chromosomal interfaces and intra-chromosomal A/B interfaces. For all domains defined by field variables $\boldsymbol{\varphi} = \{\varphi_0, \{\phi_i\}_{i=1,...,N}, \psi\}$ we assume a simple Landau-Ginzburg form including double well bulk free energy and surface contributions: $\int_\Omega d\Omega \left[f_{coex}(\boldsymbol{\varphi}) + \frac{\epsilon_{\boldsymbol{\varphi}}^2}{2} (\nabla \boldsymbol{\varphi})^2 \right]$. Where Ω is the domain of

the simulation, and ϵ_φ interfacial thickness parameter and f_{coex} is the free energy determ that maintains coexistence between two chromsomal phases . The restriction term $F_R[\boldsymbol{\varphi}]$ establishes chromosomal territories in the nucleus by penalizing the spatial overlap between chromosomal domains described by field variables ϕ_i. The free energy penalties for excluded volume interactions are introduced via positive volume overlap terms $\beta_{ij}\int_\Omega d\boldsymbol{\Omega} h(\phi_i)h(\phi_j)$ between different domains. The $h(\varphi_i)$ functions are standard polynomial forms for approximating volumes of different domains, and can be found in SI. The strength of interaction between different chromatin and nuclear domains are dictated by the energetic prefactors β_{ij}. These prefactors quantify heterochromatin-nuclear envelope soft-excluded volume interactions $\beta_{\varphi_0\psi} = \beta_0 = const$, chromosome-chromosome soft-excluded volume interactions $\beta_{\varphi_i\varphi_j} = \beta_\varphi = const$ and euchromatin-heterochromatin mixing affinity $\beta_{\psi\varphi_i} = \beta_\psi$ (See SI for numeric values of all the coefficients). The mixing affinity term β_ψ is varied extensively during simulations for investigating the impact of A/B type interactions on nuclear morphology and kinetics of chromatin reorganization during nuclear remodeling processes.

The growth free energy term $F_G[\boldsymbol{\varphi}]$ controls the volume growth/shrinking of chromosomal territories upon nuclear volume changes. The growth terms are defined via the harmonic restraint $\alpha_i(V_i - \bar{V}_i)^2$ which favors stable domain size $\bar{V}_i$ and the energetic prefactor α_i govern the strength of domain localization. The $F_I[\varphi_0,\psi]$ term accounts for heterochromatin-lamina interactions giving rise to the so called lamina associating domains (LADs) formed by heterochromatin regions (38). LADs have significant nuclear presence and are localized near the inner nuclear membranes in most of the mammalian nuclei. We model this aspect of nuclear architecture by a strong membrane affinity term which keeps heterochromatin preferentially clustered in the vicinity of the membrane region. This preferential interaction of heterochromatin with nuclear lamina is realized via $F_I[\varphi_0,\psi] = \gamma\int_\Omega d\boldsymbol{\Omega}\nabla h(\varphi_0)\cdot\nabla h(\psi)$ gradient term. Where γ is a binding affinity coefficient quantifying how strong heterochromatin is "attracted to" nuclear lamina or nuclear envelope relative to intra-chromosomal interactions.

After specifying the full free energy functional of nucleus the dynamic equations can be written for each phase-field variables using an Allen-Cahn prescription (39):

$$\begin{aligned}\frac{\partial\varphi_0}{\partial t} &= -L_{\varphi_0}\frac{\delta F[\boldsymbol{\varphi}]}{\delta\varphi_0},\\ \frac{\partial\phi_i}{\partial t} &= -L_{\phi_i}\frac{\delta F[\boldsymbol{\varphi}]}{\delta\phi_i},\\ \frac{\partial\psi}{\partial t} &= -L_\psi\frac{\delta F[\boldsymbol{\varphi}]}{\delta\psi} + \eta_\psi(\mathbf{r},t)\end{aligned} \qquad \textbf{(2)}$$

The term η_ψ accounts for fluctuations at the boundaries of euchromatin/heterochromatin islands due to finite size nature of droplets. The fluctuations are modeled as Brownian noise: $\langle\eta_\psi(\mathbf{r},t)\,\eta_\psi(\mathbf{r}',t')\rangle = A_p\delta(\mathbf{r}-\mathbf{r}')\,\delta(t-t')$ where the amplitude of noise $A_p = 2k_BT_{eff}L_\psi$ sets the "effective temperature" T_{eff} of the nucleus (32) which can be taken as a measure of ATP activity in comparisons with experiment (40, 41). We note that can in MELON framework one can readily introduce active processes and driven fluctuations in chromatin liquid droplets (40, 41). The time scale of chromatin relaxation is set by $\tau = L^{-1}$. It is well know that in different developmental stages of eukaryotic cells the dynamics of nuclear processes proceed on vastly different time-scales. Therefore, when modeling nuclear rearrangements in post-embryonic interphase we set $\tau = 5\cdot10^{-3}h$ and when modeling long-term nuclear senescence we set $\tau = 5h$ to match the relevant time-scales of attaining different nuclear morphology.

Impact of chromosome territorial affinity and heterochromatin-lamina interactions on euchromatin/heterochromatin phase separation

To illustrate the consequences of liquid behaviour and phase separation of A/B chromatin types in the nucleus we apply MELON to model drosophila nucleus in its various developmental stages. Recent experiments suggest that liquid-liquid phase separation of chromatin domains in *Drosophila melanogaster* nuclei is orchestrated by HP1a proteins, which under favorable conditions would form liquid condensates and dissolve heterochromatin regions within liquid droplets (23, 24, 42). Polymer models have shown the importance of A/B phase separation (11, 12) as one of the main driving forces behind chromatin organization in mammals. Heterochromatin-lamina interactions (43–45) are instead thought to be responsible the swithcing between conventional and inverted nuclear morphology.

Using our phase field model of the nucleus, we investigate the role of various terms in the global free energy functional in generating steady-state nuclear morphology liquid-liquid phase separation dynamics. We set the average heterochromatin content of the nucleus at 25 % corresponding to the post-embryonic stage of *Drosophila* nucleus (46). Later on, we will vary this content when investigating the impact of heterochromatin content on the dynamics of phase separation and the resulting nuclear morphology.

To describe chromatin dynamics in the nucleus quantitatively, we evaluate the temporal evolution of the summed volumes of individual chromosomes $V(t)$ and heterochromatin droplets from all chromosomes $v(t)$. The simulations that generate starting nuclear morphologies (Fig. 2AB) show that volumes $V(t)$ and $v(t)$ evolve until nucleus is filled with liquid state chromatin at which point a steady state is reached where compartments acquire well defined volumes. After coexistence between different liquid chromatin compartments is reached, we investigate how variations of interaction strengths defined in previous section alter the coexistence state of the nucleus.

We first investigate the impact of chromosome type mixing affinity β_ψ which govern the interaction range between chromatin compartments. We see that strong affinity leads to mixed states for heterochromatin droplets while weaker mixing affinity leads to fusion of heterochromatin droplets (Fig. 2CD).

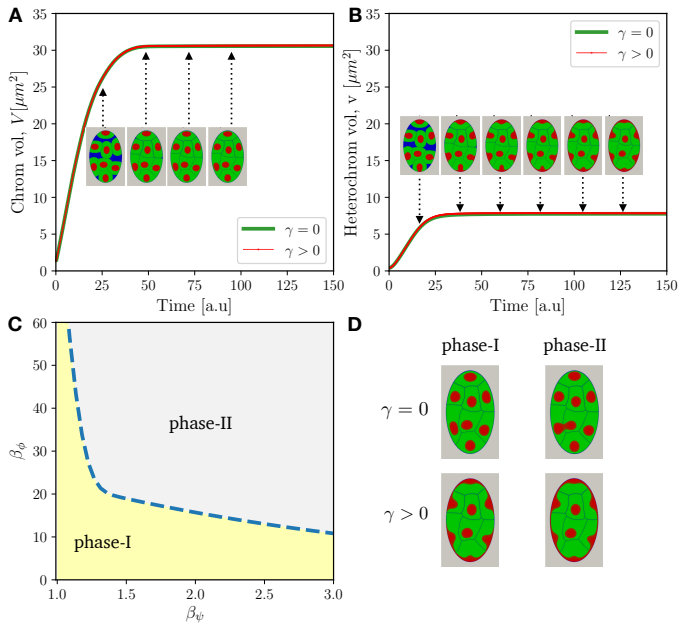

Fig. 2. Evolution of chromosomal (Fig. A)) and heterochromatin (Fig. B)) volumes in the idealized nucleus with and without heterochromatin-lamina interactions. The snapshots show the nuclear morphology at different times during the generation stage of the nucleus. The nuclear compartment is colored in blue, chromosome territory in green and heterochromatin compartment in red. (C) Phase diagram of nuclear morphology showing the impact of various constraints/affinities on liquid-liquid phase separation of A/B domains in the formation heterochromatin/euchromatin territories. Phases are defined in terms of connectivity between heterochromatin droplets (continuous vs discontinuous or piece-wise continuous variation of ψ variable, see also SI). Phase I corresponding to fully disconnected and mixed state phase II corresponding to strongly connected and de-mixed or partially de mixed states (D) Examples morphologies of different phases.

Variation of nuclear membrane lamina-heterochromatin interaction shows that nuclear morphology is significantly affected by the changes in lamina anchoring strength. This is unsurprising given the large surface area of nuclear envelope. Indeed when we set a non-zero affinity $\gamma > 0$ for the lamina interactions the heterochromatin shows pronounced localization near the nuclear envelope. In the presence of dominant lamina-heterochromatin interactions the impact of mixing affinity is now seen in different thickness of the heterochromatin belt formed around the nuclear envelope. This somewhat subtle difference is due to the competition between the lamina binding energy (negative term in the global $F[\varphi]$) and territorial interaction energy (positive term in the global $F[\varphi]$). Thus, consistent with optical microscopy observations (46, 47) and polymer simulations (43, 44), the lamina binding affinity is indeed one of the dominant physical interaction that shapes the conventional nuclear architecture.

Loss of affinity has been shown to lead to inversion of nuclear architecture, which we show is a naturally emerging behaviour of our model of the nucleus (47, 48). In the subsequent sections we show that the inversion behaviour along with its characteristic kinetics is naturally explained by "liquid-like" behaviour of chromatin.

Impact of diffusion, fluctuations and heterochromatin content on formation of liquid-chromatin compartments

In this section we study the roles of heterochromatin droplet diffusion, fluctuations and nuclear heterochromatin fraction on the kinetic of phase separation in the idealized nucleus during interphase and senescent phases. The setup of the first set of simulation is mimicking the rapid liquid like nucleoprotein droplet fusion events during interphase the dynamics of which have been observed and quantified in multiple recent experiments (23, 24, 49). *In vivo*, heterochromatin droplets and organelles display shape and size fluctuations because of both thermal fluctuations in the and active, ATP-driven motor activity in the nucleoplasm (50). In the present scheme of MELON framework, we model fluctuations by a thermal noise term which accounts for the fluctuations of finite sized droplets in an effective manner. Introduction of fluctuation has allowed us to quantify how "effective temperature" in the nucleus impacts the kinetics of phase separation. To this end we have carried out simulations with fixed nuclear volume while varying fluctuation amplitude values.

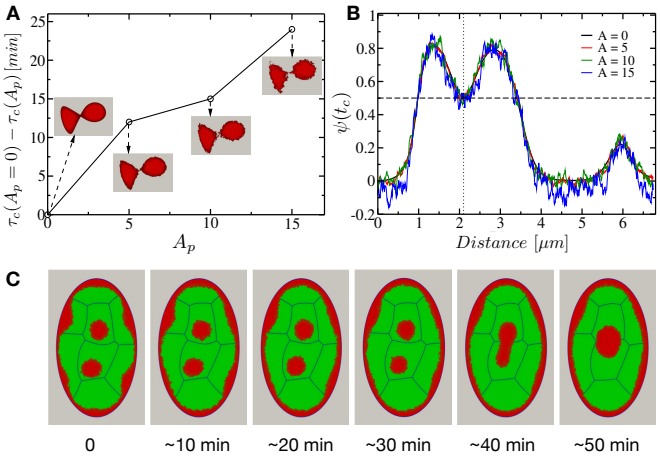

Fig. 3. Impact of euchromatin/heterochromatin boundary fluctuations on the heterochromatin droplet fusion dynamics. Shown are (A) Profile of droplet fusion time as a function of droplet fluctuation amplitude (B) The fluctuation profile along the heterochromatin order parameter (C) Representative snapshot of droplet fusion dynamics for $A_p = 10$ amplitude and post-embryonic interphase cycle for which chromatin relaxation timescale is set: $\tau = L^{-1} = 5 \cdot 10^{-3} h$

We find that passive fluctuations lead to enhancement of liquid droplet contact and fusion events which in turn enhance the kinetics of phase separation in the nucleus (Fig. 3AB). Thus, the fluctuation amplitude of heterochromatin/euchromatin interfaces effectively increases the capture radius or diffusion coefficient of the liquid droplets (Fig. 3AB). Finally the comparison with experiment shows that liquid state model of chromatin in MELON framework accurately capture the nuclear coalescence profiles and the detailed time-lapse and contours of droplet fusion events (Fig. 3BC).

Next we fix the fluctuation amplitude of droplets at fixed moderate value and consider large scale nuclear reorganization processes which are initiated upon severing the lamina and heterochromatin. These simulations would serve as a

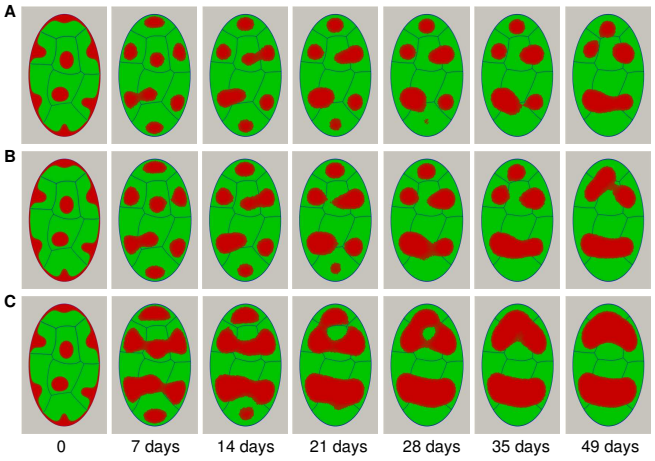

Fig. 4. Impact of heterochromatin volume fraction on the nuclear compartment reorganization with fixed nuclear size. Shown are nuclear morphologies generated with different heterochromatin contents: (A) $\rho = 25\%$ (B) 30% and (C) $\rho = 45\%$. Simulations are initiated by terminating Lamina-heterochromatin interaction and the time scale of chromatin relaxation is set for modeling nuclear senescence and inversion $\tau = L^{-1} = 5h$. $A_p = 5$ of mammalian nuclei (46)

point of comparison with nuclear volume remodeling simulations of senescence and inversion reported in the next section. Starting from a conventional nuclear morphology with 25% of heterochromatin fraction content, we monitor droplet fusion leading to partial phase separation of heterochromatin. Consistent with the microscopy experiments, the conventional structure is with sequential displacement of heterochromatin towards the center of the nucleus (Fig. 4A). During the reorganization stage, the adjacent heterochromatin droplets fuse together thereby reducing in the number of chromocenters in the nucleus (Fig. 4A)). To predict the impact of heterochromatin mobility and its fraction in the nucleus on phase separation kinetics, we performed simulations with different values of heterochromatin fractions and different diffusion coefficients. To do this, we assume that during the nuclear reorganization the heterochromatin continue growing to reach the prescribed fraction. Indeed, changing the heterochromatin fraction in conventional nuclear architecture to a newly prescribed fraction in inverted architecture should not impact strongly the displacement and fusion of heterochromatin droplets because the growth kinetics of heterochromatin is very fast with respect to heterochromatin mobility. Figures 4(B,C) represent the inverted nuclear architecture obtained for 30% and 45% of heterochromatin fraction content in the nucleus. As one would expect the higher heterochromatin content leads to faster phase separation associated with a decrease in the clustered heterochromatin number. The displacement of the heterochromatin droplets within the nucleus is controlled by the diffusion which the velocity is related to the thickness of euchromatin-heterochromatin interfacial region. The simulation results performed for a given heterochromatin fraction (30%) and a fixed nuclear volume showed that increasing the diffusion coefficient accelerate the fusion of heterochromatin droplets to form two clusters at steady-state of nuclear morphology for a higher value (Fig. S3). Additionally, we find there to be a critical threshold exceeding of which leads to fully phase separated morphology given reasonable diffusion constants and absence of any desegregating lamina-heterochromatin interactions.

Interplay between chromatin phase separation and nuclear volume remodeling accompanying senescence

The cell nucleus is subject to continuous remodeling activity changing volume, shape or internal organization in response to variety of external or internal signals. During the interphase, eukaryotic nuclei undergo steady expansion; during senescence (51) and embryonic development of rod cells (46, 47), however, nucleus can lose lamina-heterochromatin affinity and undergo large-scale redistribution of chromatin where heterochromatin becomes concentrated in the center of the nucleus. This large scale chromatin remodeling is often accompanied by shrinking of nuclear volume (47). Given the frequency in which nuclear volume/shape change and chromatin reorganization happen together, one may expect there to be robust mechanisms tuned with volume drift and fluctuations.

Phase separation of chromatin domains provides one such robust mechanism for rapid mobilization of large section of genome with predictable dependence on volume changes . In this context it is therefore worthwhile to investigate in detail how the kinetics of chromatin phase separation couples with the remodeling of nuclear volume.

To this end we have carried out simulations that mimic processes of nuclear senescence and inversion happening on the time-scale of days and resulting in dramatic change in nuclear volume and euchromatin/heterochromatin.

Within the current MELON framework, remodelling of the nuclear volume is simulated by uniaxial slow compression/expansion of membrane boundaries which allows the liquid chromatin compartments to expand/contract. The volume remodeling processes considered are all propagated at constant rate which is taken to be much slower than any of the intra-nuclear diffusion time scales: $\tau_{remod} = L_{\varphi_0}^{-1} \ll \tau_{A/B} = L_{\psi}^{-1}$. In this work we did not consider anisotropic deformations and fluctuations of the nuclear envelope (52) which certainly could be an interesting question that merits separate investigation.

The figure 5 shows the impact of nuclear volume changes on chromatin reorganization dynamics in the absence of heterochromatin-lamina interactions. We see that in all cases heterochromatin/euchromatin distribution driven toward completely phase separated states with heterochromatin accumulating in the vicinity of the nuclear core. However, the kinetics and morphology of this transition are markedly different relative to constant volume case of the previous section. This shows that chromatin diffusion rates and volume remodelling rates can be in a tug of war with each other. Additionally, we see that the chromosome territories can remain well separated during remodeling of nuclear volume which is suggesting that coexistence of key sub-nuclear compartmentalization of A/B types with optimal affinity can be made robust to volume remodeling.

To quantify the dynamics of heterochromatin/euchromatin phase separation, we have investigated how the number of heterochromatin clusters vary with target nuclear volume while keeping remodeling times fixed. The results show that the value of final volume leads to more rapid phase separation because in smaller nuclear volumes the encounter rates of heterochromatin droplets are higher (Fig. 6). Indeed, the distance between two regions occupied by heterochromatin becomes small when the nuclear volume decreases so the fusion between them becomes more favorable. Since the relaxation time of the nuclear envelope ($L_{\varphi_0} = const$) is being kept constant it is also interesting to evaluate the characteristic time of relaxation of heterochromatin domains in order to assess how much the dynamics of internal chromatin motions are affected. We find that the chromosome territories relaxed to their equilibrium volume with a nearly same relaxation time of the nucleus whereas the heterochromatin domains relaxed faster (Fig 6 and Table S1).

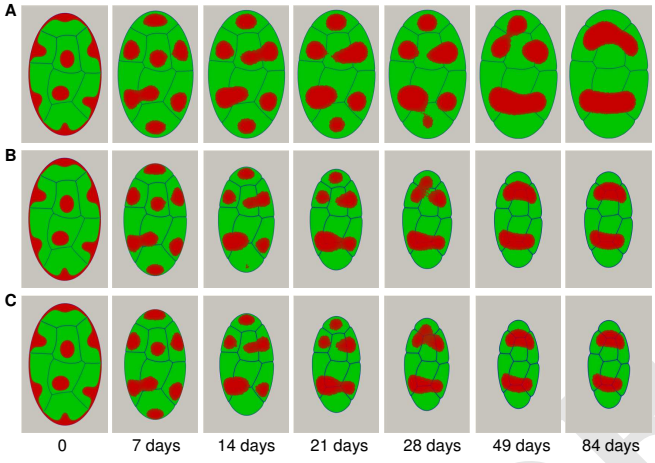

Fig. 5. Impact of nuclear volume remodeling on euchromatin/heterochromatin phase separation. Shown are simulations tat remodel nuclear volume by (A) nuclear growth with 10% of volume expansion (B) uniform nuclear compression of oblate nuclear envelope by 40% and (C) Nuclear compression by 50%. Overall heterochromatin fraction content in the nucleus is fixed at 30%.

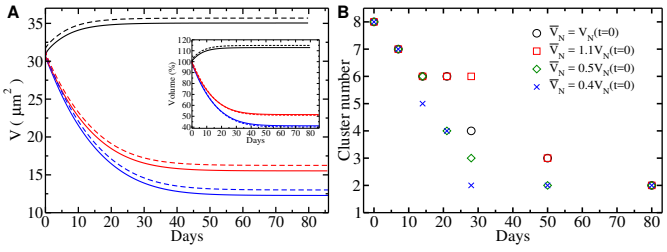

Fig. 6. (A) Volume relaxation profiles of chromosomes (solid lines) and nucleus as a whole (dashed lines) as a function of remodeling time. The color code show different target of steady-state nuclear volumes corresponding to 10% of volume expansion (black lines), volume compression by 50% (red lines) and volume compression by 40% (blue lines). (B) Temporal evolution of the number of heterochromatin cluster in the cell's nucleus during the reorganization process with different target steady-state nuclear volumes $\bar{V}_N$. All simulations of the nuclear volume remodelling were initiated by terminating heterochromatin-lamina interaction term to mimic processes of senescence and nuclear inversion. The heterochromatin fraction content in the nucleus is fixed to 30%.

Likewise, the diffusion rates and rate of volume reduction lead to a nearly uniform acceleration of the dynamics of droplet fusion events. We see that nuclear growth works against phase separation and in principle can slow it down or arrest it for some parameter regimes. Based on experimental observations (48), the time required for the complete transformation of the conventional architecture of mammalian nuclei to inverted morphology is predicted to take on the order of ~ 30 days with the corresponding heterochromatin cluster number estimated to be 2-3. The results with embryonic time scale adopted in this work are thus agreeing quantitatively with the experiments (48).

In the case of nuclear inversion, we find that while the rate of phase separation is different for heterochromatin fractions (Fig. S4, Fig. S5) and diffusion rates (Fig. S6), and the final nuclear morphology is nearly identical which is to be expected from the nature of phase separation and the thermodynamic stability of the final steady state. The reorganization process however takes place via different pathways and it may be beneficial for genetic processes to have this heterogeneity while ensuring robustness of target thermodynamic phases.

Finally we have explored the conditions under which heterochromatin domains merge into single cluster which is commonly seen in rod cells upon complete nuclear inversion (Fig. 7). Scanning phase space of nuclear morphology along the heterochromatin density axis (See SI) we have found that specific condition favoring single cluster formation is having at least 50% heterochroamtin content which in MELON framework would corresponds to combined constitutive and faculatative heterochromatin content.

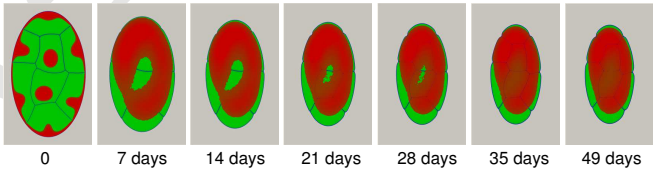

Fig. 7. An example of single heterochromatic cluster formation. Heterochromatin fraction in the nucleus is elevated to 60% to account for the existence of high combined facutlative and consitutive heterochromatin. We have used ~ 10 times high diffusion coefficient (relative to simulations in Figs 2-6) to accelerate phase separation.

Discussion

In recent years there has been an increasing interest for the liquid-like behaviour of chromatin, which has been bolstered by several experiments (20, 23, 24, 49, 53, 54), theoretical investigations (55–58) as well as computer simulations (12, 26). Despite the complexity of the polymeric medium and of the active processes operating on chromatin at the microscopic scales, the dynamical behaviour of chromatin at the nuclear scale is reminiscent of viscoelastic fluids (12). A natural question emerging from these observations of chromatin dynamics is: how much of large-scale nuclear processes such as development, aging, disease propagation could be explained just by the liquid-like behavior of chromatin? To answer this question we have developed the MEsoscale Liquid mOdel of Nucleus(MELON), a novel computational frame-

work where chromatin is resolved as complex fluid mixture composed of epigenetically colored components. Using this model, we find that a fluid description of chromatin combined with basic facts about nuclear architecture, including existence of chromosomal territories, A/B epigenetic type interactions and Lamina-heterochromatin anchoring leads to life-like nuclear morphologies. Application of the MELON framework to *Drosophila* nucleus at different developmental stages of the nucleus, such as interphase, long-time senescence and inversion reveals a rich interplay between liquid-liquid phase separation, nucleation and droplet fluctuations. We would like to further emphasize that the generic nature of the model and the minimal assumptions that we have built into it allows one to draw conclusion that we believe should be generally applicable for wide variety of eukaryotic nuclei and not just for the *Drosophila* nucleus. Particularly, our study finds that a significant role is played by surface tension and lamina-heterochromatin interactions in determining large-scale chromatin rearrangements. Our study introduces an innovative approach for studying micron-scale chromatin dynamics; we foresee that further development of the method here introduced-the MELON framework-will shed new light on the micro-rheology, the diffusive behavior and the hydrodynamics of nuclear chromatin.

ACKNOWLEDGEMENTS

DAP and RL acknowledges useful discussions with Xueyu Song and Jim Evans. DAP is grateful for the financial support from Caldwell foundation of Iowa State. M.D.P's research is supported by the Center for Theoretical Biological Physics sponsored by the National Science Foundation (Grants PHY-1427654 and NSF-CHE-1614101) and by the Welch Foundation (Grant C-1792). All the simulations in the paper were carried out using NSF' XSEDE allocation on Stampede2 machine.

Bibliography

1. Bruce Alberts. *Molecular biology of the cell*. Garland Science, Taylor and Francis Group, New York, NY, 2015. ISBN 978-0815344322.
2. Rob Phillips. *Physical biology of the cell*. Garland Science, London New York, NY, 2013. ISBN 978-0815344506.
3. Erez Lieberman-Aiden, Nynke L Van Berkum, Louise Williams, Maxim Imakaev, Tobias Ragoczy, Agnes Telling, Ido Amit, Bryan R Lajoie, Peter J Sabo, Michael O Dorschner, et al. Comprehensive mapping of long-range interactions reveals folding principles of the human genome. *science*, 326(5950):289–293, 2009.
4. Lauren Meldi and Jason H Brickner. Compartmentalization of the nucleus. *Trends in cell biology*, 21(12):701–708, 2011.
5. Suhas SP Rao, Miriam H Huntley, Neva C Durand, Elena K Stamenova, Ivan D Bochkov, James T Robinson, Adrian L Sanborn, Ido Machol, Arina D Omer, Eric S Lander, et al. A 3d map of the human genome at kilobase resolution reveals principles of chromatin looping. *Cell*, 159(7):1665–1680, 2014.
6. Emil Heitz. Das heterochromatin der moose. *Jahrbucher fur Wissenschaftliche Botanik*, 69: 762–818, 1929.
7. Ryosuke Imai, Tadasu Nozaki, Tomomi Tani, Kazunari Kaizu, Kayo Hibino, Satoru Ide, Sachiko Tamura, Koichi Takahashi, Michael Shribak, and Kazuhiro Maeshima. Density imaging of heterochromatin in live cells using orientation-independent-dic microscopy. *Molecular biology of the cell*, 28(23):3349–3359, 2017.
8. Jonathan B Grimm, Brian P English, Jiji Chen, Joel P Slaughter, Zhengjian Zhang, Andrey Revyakin, Ronak Patel, John J Macklin, Davide Normanno, Robert H Singer, et al. A general method to improve fluorophores for live-cell and single-molecule microscopy. *Nature methods*, 12(3):244, 2015.
9. Horng D Ou, Sébastien Phan, Thomas J Deerinck, Andrea Thor, Mark H Ellisman, and Clodagh C O 'shea. ChromEMT: Visualizing 3D chromatin structure and compaction in interphase and mitotic cells. *Science*, 357:370, 2017.
10. Michele Di Pierro, Bin Zhang, Erez Lieberman Aiden, Peter G Wolynes, and José N Onuchic. Transferable model for chromosome architecture. *Proceedings of the National Academy of Sciences*, 113(43):12168–12173, 2016.
11. Michele Di Pierro, Ryan R Cheng, Erez Lieberman Aiden, Peter G Wolynes, and José N Onuchic. De novo prediction of human chromosome structures: Epigenetic marking patterns encode genome architecture. *Proceedings of the National Academy of Sciences*, page 201714980, 2017.
12. Michele Di Pierro, Davit A Potoyan, Peter G Wolynes, and José N Onuchic. Anomalous diffusion, spatial coherence, and viscoelasticity from the energy landscape of human chromosomes. *Proc. Natl. Acad. Sci. U. S. A.*, July 2018.
13. Mariano Barbieri, Mita Chotalia, James Fraser, Liron-Mark Lavitas, Josée Dostie, Ana Pombo, and Mario Nicodemi. Complexity of chromatin folding is captured by the strings and binders switch model. *Proceedings of the National Academy of Sciences*, 109(40): 16173–16178, 2012.
14. Daniel Jost, Pascal Carrivain, Giacomo Cavalli, and Cédric Vaillant. Modeling epigenome folding: formation and dynamics of topologically associated chromatin domains. *Nucleic acids research*, 42(15):9553–9561, 2014.
15. Quinn MacPherson, Bruno Beltran, and Andrew J Spakowitz. Bottom–up modeling of chromatin segregation due to epigenetic modifications. *Proceedings of the National Academy of Sciences*, 115(50):12739–12744, 2018.
16. Pilong Li, Sudeep Banjade, Hui-Chun Cheng, Soyeon Kim, Baoyu Chen, Liang Guo, Marc Llaguno, Javoris V Hollingsworth, David S King, Salman F Banani, et al. Phase transitions in the assembly of multivalent signalling proteins. *Nature*, 483(7389):336, 2012.
17. Clifford P Brangwynne, Christian R Eckmann, David S Courson, Agata Rybarska, Carsten Hoege, Jöbin Gharakhani, Frank Jülicher, and Anthony A Hyman. Germline p granules are liquid droplets that localize by controlled dissolution/condensation. *Science*, 324(5935): 1729–1732, 2009.
18. Sudeep Banjade and Michael K Rosen. Phase transitions of multivalent proteins can promote clustering of membrane receptors. *Elife*, 3:e04123, 2014.
19. Clifford P Brangwynne, Timothy J Mitchison, and Anthony A Hyman. Active liquid-like behavior of nucleoli determines their size and shape in xenopus laevis oocytes. *Proceedings of the National Academy of Sciences*, 108(11):4334–4339, 2011.
20. Clifford P Brangwynne, Peter Tompa, and Rohit V Pappu. Polymer physics of intracellular phase transitions. *Nature Physics*, 11(11):899, 2015.
21. Vladimir N Uversky. Protein intrinsic disorder-based liquid–liquid phase transitions in biological systems: Complex coacervates and membrane-less organelles. *Advances in colloid and interface science*, 239:97–114, 2017.
22. Steven Boeynaems, Simon Alberti, Nicolas L Fawzi, Tanja Mittag, Magdalini Polymenidou, Frederic Rousseau, Joost Schymkowitz, James Shorter, Benjamin Wolozin, Ludo Van Den Bosch, et al. Protein phase separation: a new phase in cell biology. *Trends in cell biology*, 28(6):420–435, 2018.
23. Amy R Strom, Alexander V Emelyanov, Mustafa Mir, Dmitry V Fyodorov, Xavier Darzacq, and Gary H Karpen. Phase separation drives heterochromatin domain formation. *Nature*, 2017.
24. Adam G Larson, Daniel Elnatan, Madeline M Keenen, Michael J Trnka, Jonathan B Johnston, Alma L Burlingame, David A Agard, Sy Redding, and Geeta J Narlikar. Liquid droplet formation by HP1α suggests a role for phase separation in heterochromatin. *Nature*, 547 (7662):236–240, June 2017.
25. Yongdae Shin and Clifford P Brangwynne. Liquid phase condensation in cell physiology and disease. *Science*, 357(6357), September 2017.
26. Lei Liu, Guang Shi, D Thirumalai, and Changbong Hyeon. Chain organization of human interphase chromosome determines the spatiotemporal dynamics of chromatin loci. *PLoS computational biology*, 14(12):e1006617, 2018.
27. Johannes Nuebler, Geoffrey Fudenberg, Maxim Imakaev, Nezar Abdennur, and Leonid A Mirny. Chromatin organization by an interplay of loop extrusion and compartmental segregation. *Proceedings of the National Academy of Sciences*, 115(29):E6697–E6706, 2018.
28. Adrian L Sanborn, Suhas S P Rao, Su-Chen Huang, Neva C Durand, Miriam H Huntley, Andrew I Jewett, Ivan D Bochkov, Dharmaraj Chinnappan, Ashok Cutkosky, Jian Li, Kristopher P Geeting, Andreas Gnirke, Alexandre Melnikov, Doug McKenna, Elena K Stamenova, Eric S Lander, and Erez Lieberman Aiden. Chromatin extrusion explains key features of loop and domain formation in wild-type and engineered genomes. *Proc. Natl. Acad. Sci. U. S. A.*, 112(47):E6456–65, November 2015.
29. I Bronshtein, E Kepten, I Kanter, S Berezin, M Lindner, Abena B Redwood, S Mai, S Gonzalo, R Foisner, Y Shav-Tal, and Y Garini. Loss of lamin a function increases chromatin dynamics in the nuclear interior. *Nat. Commun.*, 6:8044, August 2015.
30. Joseph S Lucas, Yaojun Zhang, Olga K Dudko, and Cornelis Murre. 3d trajectories adopted by coding and regulatory dna elements: first-passage times for genomic interactions. *Cell*, 158(2):339–352, 2014.
31. Alexandra Zidovska, David A Weitz, and Timothy J Mitchison. Micron-scale coherence in interphase chromatin dynamics. *Proceedings of the National Academy of Sciences*, 110 (39):15555–15560, 2013.
32. Robijn Bruinsma, Alexander Y Grosberg, Yitzhak Rabin, and Alexandra Zidovska. Chromatin hydrodynamics. *Biophys. J.*, 106(9):1871–1881, 2014.
33. Makiko Nonomura. Study on multicellular systems using a phase field model. *PloS one*, 7 (4):e33501, 2012.
34. S Seirin Lee, S Tashiro, A Awazu, and R Kobayashi. A new application of the phase-field method for understanding the mechanisms of nuclear architecture reorganization. *J. Math. Biol.*, 2017.
35. Dan Deviri, Dennis E Discher, and Sam A Safran. Rupture dynamics and chromatin herniation in deformed nuclei. *Biophys. J.*, 113(5):1060–1071, September 2017.
36. Shamik Sen, Adam J Engler, and Dennis E Discher. Matrix strains induced by cells: computing how far cells can feel. *Cellular and molecular bioengineering*, 2(1):39–48, 2009.
37. Miloš Knežević, Hongda Jiang, and Shenshen Wang. Active tuning of synaptic patterns enhances immune discrimination. *Physical review letters*, 121(23):238101, 2018.
38. Bas van Steensel and Andrew S Belmont. Lamina-Associated domains: Links with chromosome architecture, heterochromatin, and gene repression. *Cell*, 169(5):780–791, May 2017.
39. S. M Allen and J.W Cahn. microscopic theory for antiphase boundary motion and its application to antiphase domain coarsening. *Acta. Metall.*, 27:1084, 1979.
40. David Saintillan, Michael J Shelley, and Alexandra Zidovska. Extensile motor activity drives coherent motions in a model of interphase chromatin. *Proceedings of the National Academy of Sciences*, 115(45):11442–11447, 2018.
41. David Zwicker, Johannes Baumgart, Stefanie Redemann, Thomas Müller-Reichert, Anthony A. Hyman, and Frank Jülicher. Positioning of particles in active droplets. *Phys. Rev. Lett.*, 121:158102, Oct 2018. doi: 10.1103/PhysRevLett.121.158102.
42. Adam G Larson and Geeta J Narlikar. The role of phase separation in heterochromatin

formation, function, and regulation. *Biochemistry*, 57(17):2540–2548, May 2018.

43. Nicholas Allen Kinney, Igor V Sharakhov, and Alexey V Onufriev. Chromosome–nuclear envelope attachments affect interphase chromosome territories and entanglement. *Epigenetics & chromatin*, 11(1):3, 2018.
44. Michael Chiang, Davide Michieletto, Chris A Brackley, Nattaphong Rattanavirotkul, Hisham Mohammed, Davide Marenduzzo, and Tamir Chandra. Lamina and heterochromatin direct chromosome organisation in senescence and progeria. *bioRxiv*, page 468561, 2018.
45. Martin Falk, Yana Feodorova, Natasha Naumova, Maxim Imakaev, Bryan R Lajoie, Heinrich Leonhardt, Boris Joffe, Job Dekker, Geoffrey Fudenberg, Irina Solovei, et al. Heterochromatin drives organization of conventional and inverted nuclei. *bioRxiv*, page 244038, 2018.
46. Irina Solovei, Katharina Thanisch, and Yana Feodorova. How to rule the nucleus: divide et impera. *Curr. Opin. Cell Biol.*, 40:47–59, 2016.
47. Irina Solovei, Audrey S Wang, Katharina Thanisch, Christine S Schmidt, Stefan Krebs, Monika Zwerger, Tatiana V Cohen, Didier Devys, Roland Foisner, Leo Peichl, Harald Herrmann, Helmut Blum, Dieter Engelkamp, Colin L Stewart, Heinrich Leonhardt, and Boris Joffe. LBR and lamin A/C sequentially tether peripheral heterochromatin and inversely regulate differentiation. *Cell*, 152(3):584–598, January 2013.
48. Irina Solovei, Moritz Kreysing, Christian Lanctôt, Süleyman Kösem, Leo Peichl, Thomas Cremer, Jochen Guck, and Boris Joffe. Nuclear architecture of rod photoreceptor cells adapts to vision in mammalian evolution. *Cell*, 137(2):356–368, April 2009.
49. Christina M. Caragine, Shannon C. Haley, and Alexandra Zidovska. Surface fluctuations and coalescence of nucleolar droplets in the human cell nucleus. *Phys. Rev. Lett.*, 121: 148101, Oct 2018. doi: 10.1103/PhysRevLett.121.148101.
50. Fang-Yi Chu, Shannon C Haley, Alexandra Zidovska, and David A Weitz. On the origin of shape fluctuations of the cell nucleus. *Proceedings of the National Academy of Sciences*, 114:10338–10343, 2017. doi: 10.1073/pnas.1702226114.
51. Emilie Lukášová, Aleš Kovařík, and Stanislav Kozubek. Consequences of lamin b1 and lamin b receptor downregulation in senescence. *Cells*, 7(2):11, 2018.
52. Fang-Yi Chu, Shannon C Haley, and Alexandra Zidovska. On the origin of shape fluctuations of the cell nucleus. *Proceedings of the National Academy of Sciences*, 114(39):10338–10343, 2017.
53. Marina Feric, Nilesh Vaidya, Tyler S Harmon, Diana M Mitrea, Lian Zhu, Tiffany M Richardson, Richard W Kriwacki, Rohit V Pappu, and Clifford P Brangwynne. Coexisting liquid phases underlie nucleolar subcompartments. *Cell*, 165(7):1686–1697, 2016.
54. Eric B Gibbs and Richard W Kriwacki. Linker histones as liquid-like glue for chromatin. *Proceedings of the National Academy of Sciences*, 115(47):11868–11870, 2018.
55. Kazuhiro Maeshima, Satoru Ide, Kayo Hibino, and Masaki Sasai. Liquid-like behavior of chromatin. *Current opinion in genetics & development*, 37:36–45, 2016.
56. Francisco J Iborra. Can visco-elastic phase separation, macromolecular crowding and colloidal physics explain nuclear organisation? *Theor. Biol. Med. Model.*, 4:15, April 2007.
57. Fabian Erdel and Karsten Rippe. Formation of chromatin subcompartments by phase separation. *Biophys. J.*, 114(10):2262–2270, May 2018.
58. KE Polovnikov, M Gherardi, M Cosentino-Lagomarsino, and MV Tamm. Fractal folding and medium viscoelasticity contribute jointly to chromosome dynamics. *Physical review letters*, 120(8):088101, 2018.